Supporting Information

Estimating the Melting Temperatures of Type V Deep Eutectic Solvents

Gabriel Teixeira[†], Dinis O. Abranches[†], Olga Ferreira[‡,§,*], João A. P. Coutinho[†]

[†]CICECO, Aveiro Institute of Materials, Complexo de Laboratórios Tecnológicos, University of Aveiro, Campus Universitário de Santiago, 3810-193 Aveiro, Portugal

[‡]Centro de Investigação de Montanha (CIMO), Instituto Politécnico de Bragança, Campus de Santa Apolónia, 5300-253 Bragança, Portugal

[§]Laboratório para a Sustentabilidade e Tecnologia em Regiões de Montanha, Instituto Politécnico de Bragança, Campus de Santa Apolónia, 5300-253 Bragança, Portugal

[*]Corresponding author: Olga Ferreira, E-mail address: oferreira@ipb.pt, Phone: +351 273 303 087

Figures

The absolute errors were calculated as exemplified by the double headed arrows in Figure S.1.

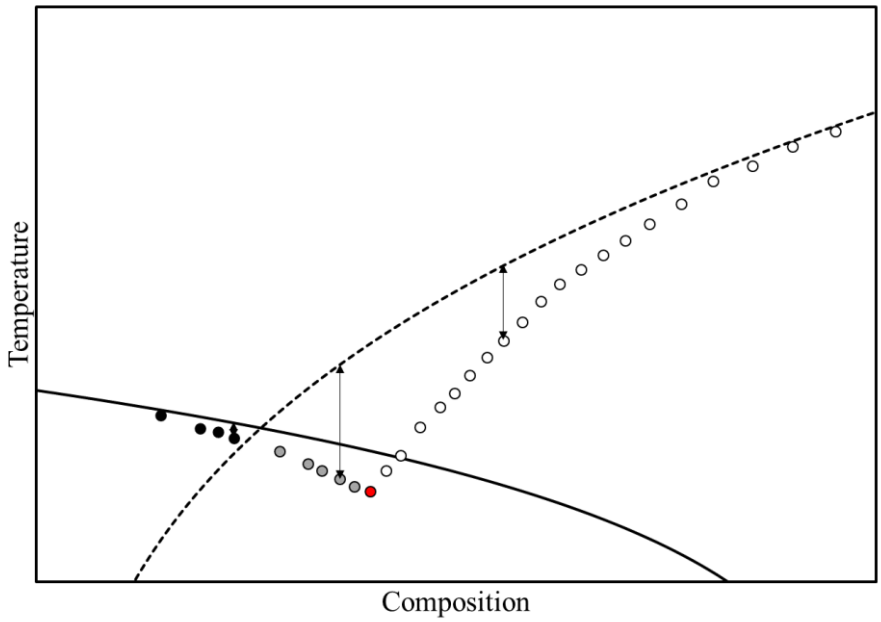

Figure S.1 – Example of the calculation of the absolute deviation between model predicted melting temperatures and experimental values.

In this work, the absolute deviations were calculated comparing the experimental data point with the maximum point predicted using the curves obtained from the SLE of both components (solid and dashed lines).

Since some eutectic mixtures can present more complex phase behaviour such as peritectic transition (i.e., myristic acid/palmitic acid [1]), solid phase partial miscibility (i.e., thymol/menthol [2]) or cocrystal formation (i.e., 3,5-dimethylphenol/menthol [3]), all gathered data were curated, leaving only the datapoints that rely solely on the pure compounds melting properties. This curation is denoted on Table S.1.

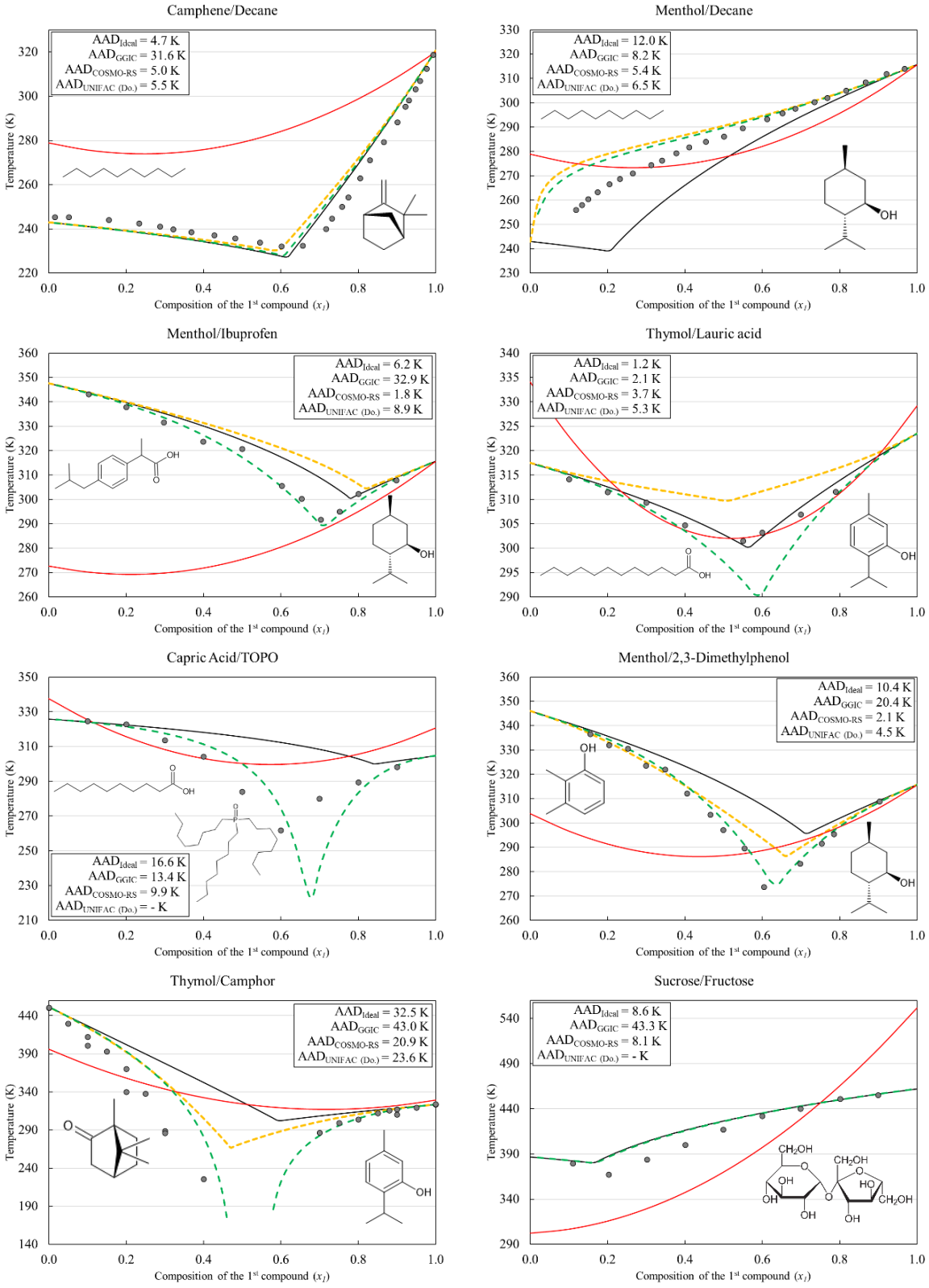

Figure S.2 – SLE diagrams of selected systems: camphene/decane, menthol/decane, menthol/ibuprofen, thymol/lauric acid, capric acid/TOPO, menthol/2,3-dimethylphenol, thymol/camphor and sucrose/fructose. Symbols represent the experimental melting temperature from literature (see Table S.1). Lines: black solid lines represent the ideal model (using Eq. (2) and γ_i=1), red solid lines represent the GGIC model, green dashed lines represent COSMO-RS (TZVP) prediction, and the yellow dashed lines represent UNIFAC (Do.) prediction.

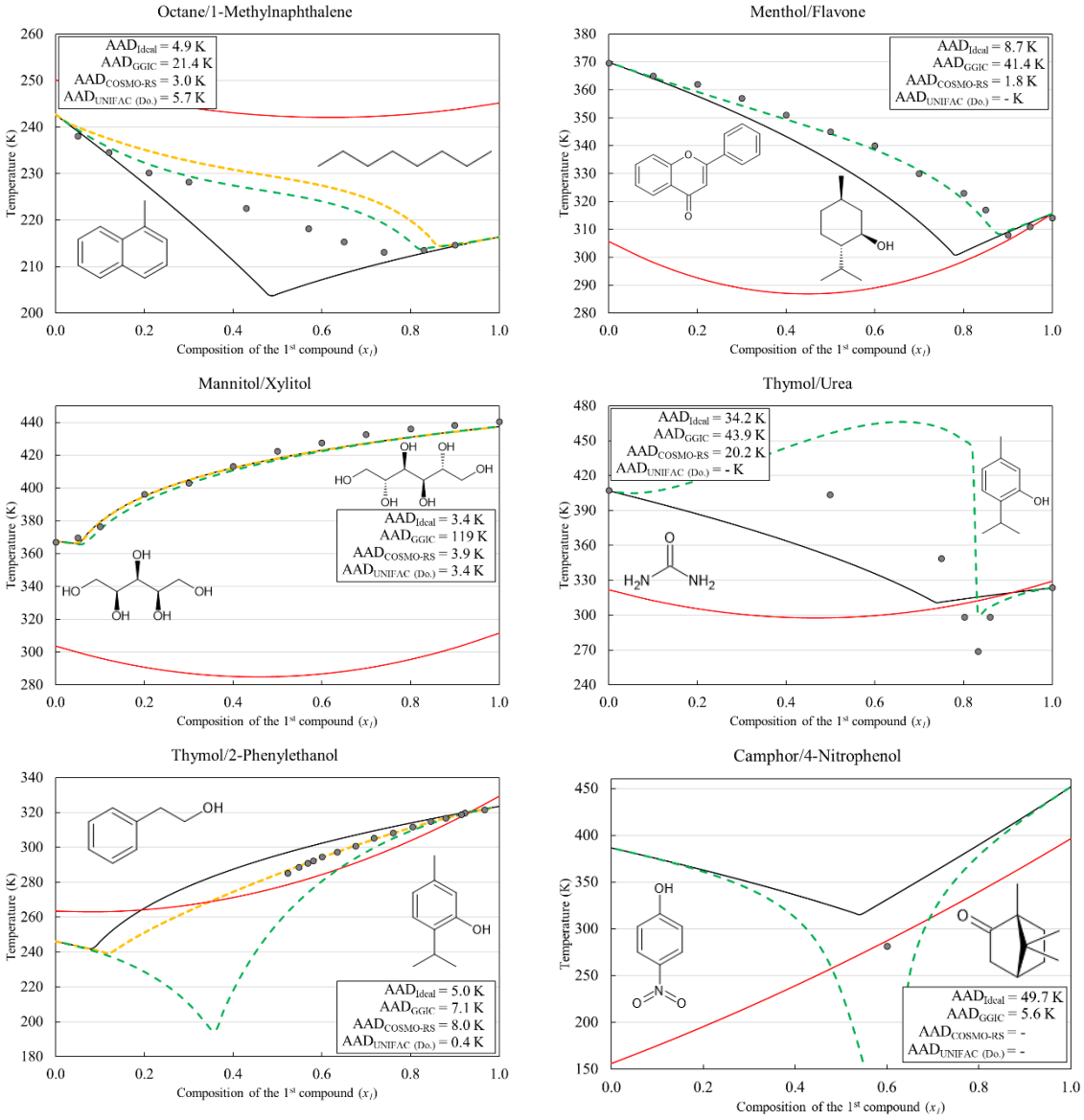

Figure S.3 - SLE diagrams of selected systems: octane/1-methylnaphthalene, menthol/flavone, mannitol/xylitol, thymol/urea, thymol/2-phenylethanol, camphor/4-nitrophenol. Symbols represent the experimental melting temperature from literature (see Table S.1). Lines: black solid lines represent the ideal model (using Eq. (2) and γ_i=1), red solid lines represent the GGIC model, green dashed lines represent COSMO-RS (TZVP) prediction, and the yellow dashed lines represent UNIFAC (Do.) prediction.

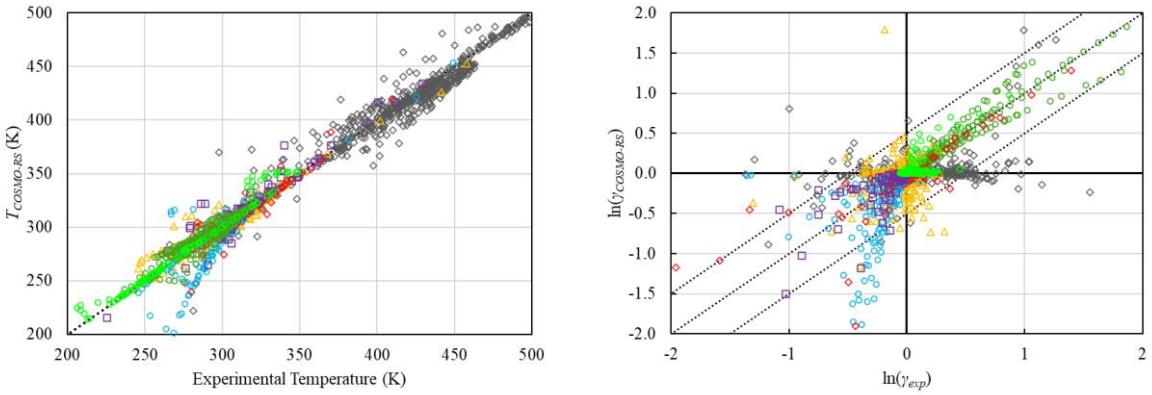

Figure S.4 – Comparison between COSMO-RS (TZVP) predictions and experimental (left) temperature and (right) activity coefficient of the studied systems. Dotted lines correspond to the ln γ ± 0.5 ln unit. Color scheme: Regular HBD- Regular HBA; Asymmetric HBD – Regular HBA; Regular HBD – Lone HBA; Lone HBA – Asymmetric HBD; Hydrocarbon mixture; Hydrocarbon+Alcohol mixture; and Polyfunctional.

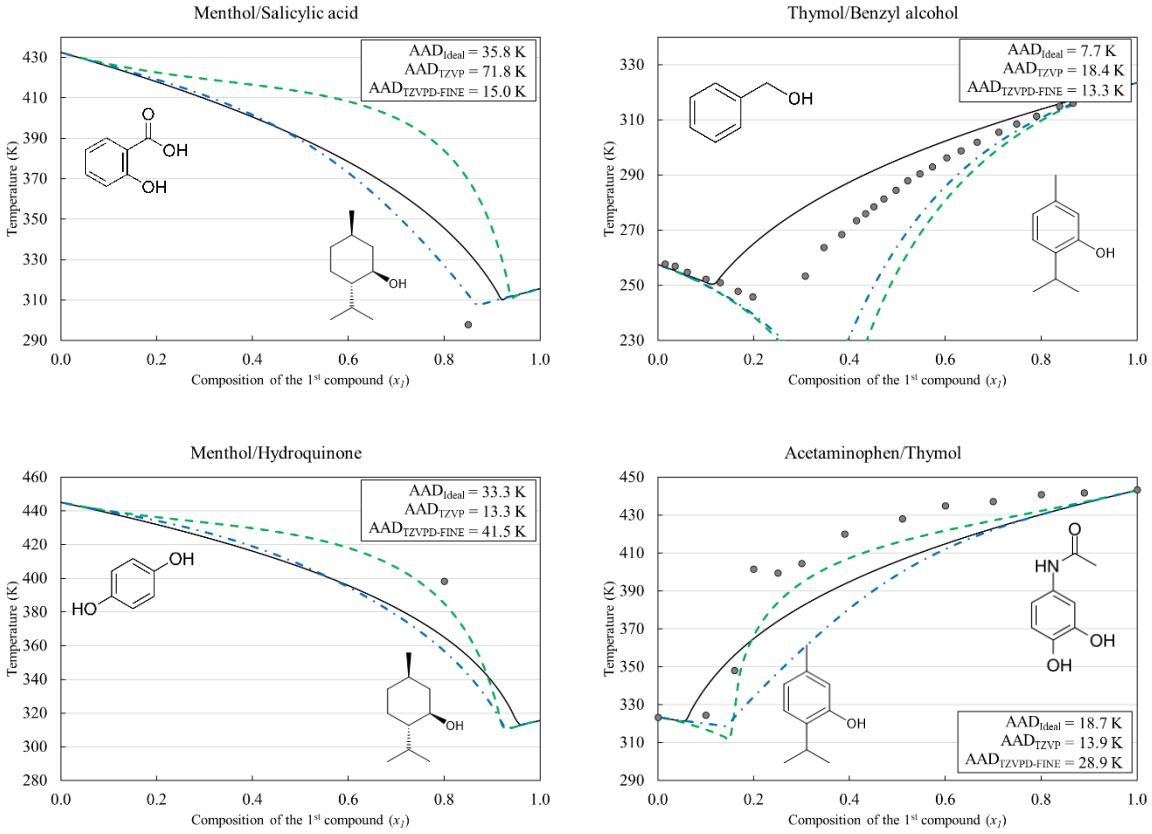

Figure S.5 – SLE diagrams of selected systems: menthol/salicylic acid; thymol/benzyl alcohol; menthol/hydroquinone; and acetaminophen/thymol. Symbols represent the experimental melting temperature from literature (see Table S.1). Lines: black solid lines represent the ideal model (using Eq. (2) and γ_i=1), green dashed lines represent COSMO-RS prediction with TZVP parametrization, and the blue point-dashed lines represent COSMO-RS prediction with TZVPD-FINE parametrization.

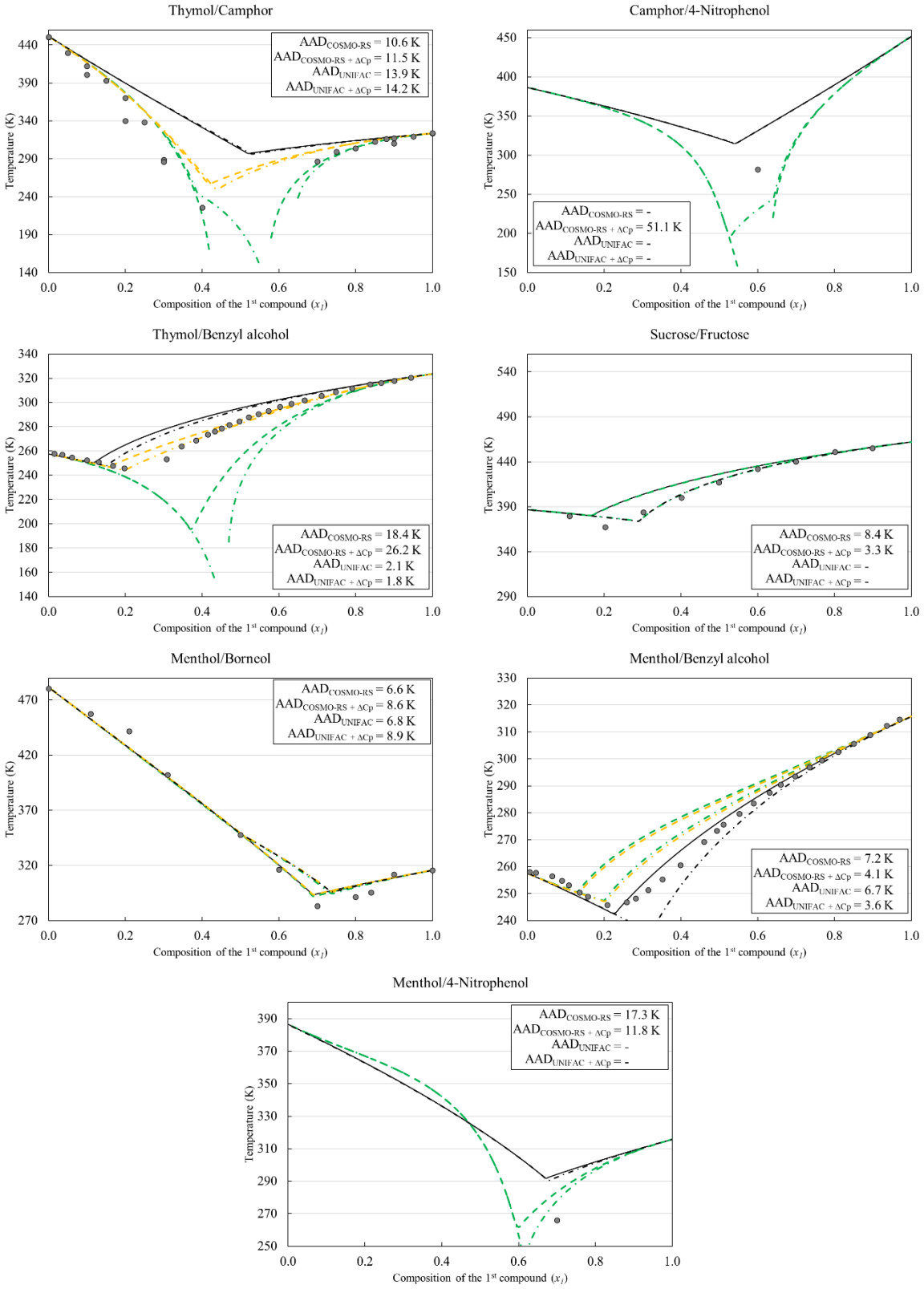

Figure S.6 - SLE diagrams of selected systems: thymol/camphor, camphor/4-nitrophenol, thymol/benzyl alcohol, sucrose/fructose, menthol/borneol, menthol/benzyl alcohol and menthol/4-nitrophenol. Symbols represent the experimental melting temperature from literature (see Table S.1). Lines: black solid lines represent the ideal model (γ_i=1) using Eq. (2), black point-dashed lines represent the ideal model (γ_i=1) using Eq. (1), green lines represent COSMO-RS prediction (TZVP), and the yellow lines represent UNIFAC (Do.) prediction, the dashed lines represent the model predictions using Eq. (2) and the point-dashed lines, using Eq. (1) and solid-solid transitions and $\Delta_m C_p$ data from the literature (see Table S.1).

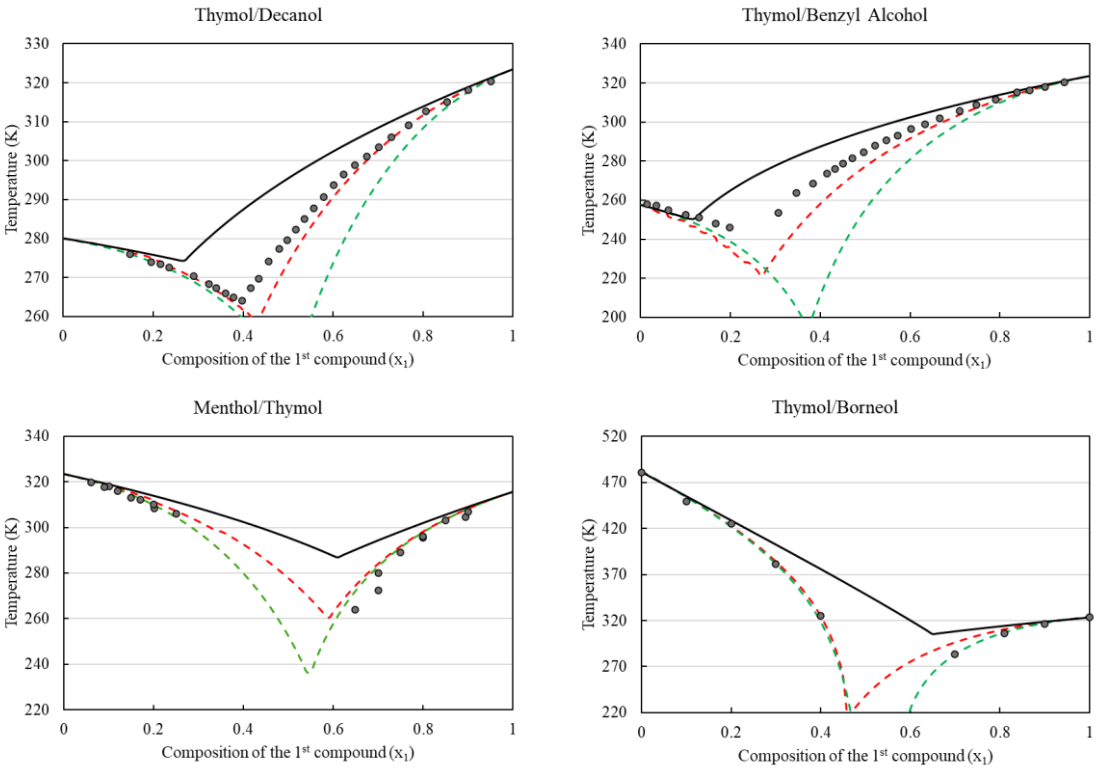

Figure S.7 – Examples of different methodologies of COSMO-RS predictions. Symbols represent the experimental melting temperature from literature (see Table S.1). Lines: black solid lines represent the ideal model (using Eq. (2) and γ_i=1); red dashed lines represent the COSMO-RS prediction with two thymol conformers; and the green dashed lines represent COSMO-RS prediction with one thymol conformer.

Tables

Table S.1 – List of binary systems studied.

System	Category	Ref.
Camphor/4-nitrophenol	Polyfunctional	4
Camphor/hydroquinone	Polyfunctional	4
Capric acid/lauric acid	HBA/HBD	1,5 *a*
Capric acid/myristic acid	HBA/HBD	6
Capric acid/palmitic acid	HBA/HBD	6
Capric acid/stearic acid	HBA/HBD	6
Capric acid/3-phenylpropionic acid	HBA/HBD	7
Capric acid/oleic acid	HBA/HBD	8
Caprylic acid/capric acid	HBA/HBD	1 *a*
Coumarin/butylated hydroxytoluene	LHBA/AHBD	4
Coumarin/thymol	LHBA/AHBD	4
Menthol/lauric acid	HBA/HBD	9
Lauric acid/myristic acid	HBA/HBD	1 *a*
Lauric acid/palmitic acid	HBA/HBD	6 *a*
Lauric acid/stearic acid	HBA/HBD	6
Menthol/ibuprofen	HBA/HBD	10 *b*
Menthol/decanol	HBA/HBD	11
Menthol/benzyl alcohol	HBA/HBD	11
Menthol/capric acid	HBA/HBD	9
Menthol/caprylic acid	HBA/HBD	9
Menthol/3-cyclohexylpropionic acid	HBA/HBD	12
Menthol/myristic acid	HBA/HBD	12
Menthol/palmitic acid	HBA/HBD	12
Menthol/3-phenylpropionic acid	HBA/HBD	12
Menthol/stearic acid	HBA/HBD	12
Menthol/4-nitrophenol	Polyfunctional	4
Menthol/butylated hydroxytoluene	HBA/AHBD	4
Menthol/hexadecanol	HBA/HBD	13
Menthol/hydroquinone	Polyfunctional	4
Menthol/octadecanol	HBA/HBD	13
Menthol/salicylic acid	Polyfunctional	4
Menthol/tetradecanol	HBA/HBD	13
Menthol/thymol	HBA/AHBD	2,4 *a*
Myristic acid/palmitic acid	HBA/HBD	1 *a*
Palmitic acid/stearic acid	HBA/HBD	1 *a*
Thymol/camphor	AHBD/LHBA	14,15
Thymol/decanol	AHBD/HBA	11
Thymol/benzyl alcohol	AHBD/HBA	11
Thymol/capric acid	HBA/HBD	9
Thymol/caprylic acid	HBA/HBD	9
Thymol/hexadecanol	AHBD/HBA	13
Thymol/ibuprofen	HBA/HBD	10 *b*
Thymol/lauric acid	HBA/HBD	9
Thymol/myristic acid	HBA/HBD	9
Thymol/octadecanol	AHBD/HBA	13
Thymol/palmitic acid	HBA/HBD	9
Thymol/stearic acid	HBA/HBD	9
Thymol/tetradecanol	AHBD/HBA	13
Trioctylphosphine oxide/capric acid	LHBA/HBD	7
Trioctylphosphine oxide/lauric acid	LHBA/HBD	16
Trioctylphosphine oxide/N,N'-dihexylthiourea	LHBA/HBD	16
Trioctylphosphine oxide/phenol	LHBA/AHBD	17
Trioctylphosphine oxide/thymol	LHBA/AHBD	7
Coumarin/salicylic acid	Polyfunctional	4

Thymol/2-cyclohexylethanol	AHBD/HBA	[11]
Thymol/decane	Alcohol/Hydrocarbon	[11]
Thymol/dodecane	Alcohol/Hydrocarbon	[18]
Thymol/dodecanol	AHBD/HBA	[18]
Thymol/2-phenylethanol	AHBD/HBA	[18]
Mannitol/meso-erythritol	Polyfunctional	[19]
Mannitol/xylitol	Polyfunctional	[19]
Mannitol/sorbitol	Polyfunctional	[19]
Maltitol/meso-erythritol	Polyfunctional	[19]
Maltitol/xylitol	Polyfunctional	[19]
Maltitol/sorbitol	Polyfunctional	[19]
Maltitol/mannitol	Polyfunctional	[19]
Thymol/flavone	AHBD/LHBA	[20]
Thymol/flavanone	AHBD/LHBA	[20]
Thymol/hesperetin	Polyfunctional	[20]
Menthol/flavone	HBD/LHBA	[20]
Menthol/flavanone	HBD/LHBA	[20]
Menthol/hesperetin	Polyfunctional	[20]
Menthol/camphor	HBD/LHBA	[14]
Menthol/borneol	HBA/HBD	[14]
Menthol/sobrerol	Polyfunctional	[14]
Thymol/borneol	AHBD/HBA	[14]
Thymol/sobrerol	Polyfunctional	[14]
Camphor/sobrerol	Polyfunctional	[14]
Borneol/sobrerol	Polyfunctional	[14]
Acetylsalicylic acid/coumarin	Polyfunctional	[21]
Acetylsalicylic acid/thymol	Polyfunctional	[21]
Ibuprofen/coumarin	HBD/LHBA	[21]
Ketoprofen/coumarin	Polyfunctional	[21]
Ketoprofen/thymol	Polyfunctional	[21]
Lidocaine/coumarin	Polyfunctional	[21]
Lidocaine/thymol	Polyfunctional	[21]
Acetaminophen/coumarin	Polyfunctional	[21]
Acetaminophen/thymol	Polyfunctional	[21]
Menthol/dodecane	Alcohol/Hydrocarbon	[18]
Menthol/dodecanol	HBA/HBD	[18]
Menthol/2-phenylethanol	HBA/HBD	[18]
Camphene/decane	Hydrocarbon Mixture	[22]
Camphene/dodecane	Hydrocarbon Mixture	[22]
Camphene/decanol	Hydrocarbon/Alcohol	[22]
Camphene/dodecanol	Hydrocarbon/Alcohol	[22]
Camphene/benzyl alcohol	Hydrocarbon/Alcohol	[22]
Camphene/2-phenylethanol	Hydrocarbon/Alcohol	[22]
Camphene/2-cyclohexylethanol	Hydrocarbon/Alcohol	[22]
Menthol/decane	Alcohol/Hydrocarbon	[11]
Octane/1-methylnaphthalene	Hydrocarbon Mixture	[23]
p-Xylene/hexadecane	Hydrocarbon Mixture	[23]
2,4,6-Trimethylphenol/2,5-dimethylphenol	HBA/HBD	[24]
Dibenzofuran/tetracosane	Hydrocarbon Mixture	[25]
Naphthalene/tetracosane	Hydrocarbon Mixture	[25]
Trioctylphosphine oxide/malonic acid	Polyfunctional	[26]
Trioctylphosphine oxide/levulinic acid	Polyfunctional	[26]
Trioctylphosphine oxide/menthol	LHBA/HBD	[27 *b*]
Naphthalene/octacosane	Hydrocarbon Mixture	[25 *b*]
Dulcitol/inositol	Polyfunctional	[28 *b*]
Mannitol/inositol	Polyfunctional	[28 *b*]
Dulcitol/mannitol	Polyfunctional	[28 *b*]
Dulcitol/sorbitol	Polyfunctional	[28 *b*]

Dulcitol/adonitol	Polyfunctional	28 *b*
Mannitol/adonitol	Polyfunctional	28 *b*
Dulcitol/arabitol	Polyfunctional	28 *b*
Mannitol/arabitol	Polyfunctional	28 *b*
Dulcitol/xylitol	Polyfunctional	28 *b*
Sucrose/glucose	Polyfunctional	29
Sucrose/fructose	Polyfunctional	29
Glucose/fructose	Polyfunctional	29
Menthol/2,3-dimethylphenol	HBA/AHBD	3
Menthol/2,5-dimethylphenol	HBA/AHBD	3
Menthol/2,6-dimethylphenol	HBA/AHBD	3
Menthol/3,4-dimethylphenol	HBA/AHBD	3
Menthol/3,5-dimethylphenol	HBA/AHBD	3
Curcumin/tyramine	Polyfunctional	30
Thymol/phenylacetic acid	HBA/HBD	31 *b*
Thymol/urea	HBA/HBD	31 *b*
Thymol/water	AHBD/HBA	31 *b*
Benzoic acid/thymol	HBA/HBD	31 *b*
Benzoic acid/caprylic acid	HBA/HBD	31 *b*
Phenylacetic acid/caprylic acid	HBA/HBD	31 *b*
Phenylacetic acid/capric acid	HBA/HBD	31 *b*
Urea/caprylic acid	HBA/HBD	31 *b*

[a] Data curated to leave only the datapoints that rely solely on the pure compounds melting properties. [b] Numerical data not available in the original publication. Data manually extracted from figures.

Table S.2 –Melting and solid–solid transition properties of the components studied.

Compound	T_m (K)	$\Delta_m H$ (kJ/mol)	$\Delta_m C_p$ (J/mol·K)	T_{SS} (K)	$\Delta_{SS} H$ (kJ/mol)
Thymol	323.5 [9]	19.65 [9]	71.75 [32]	-	-
(-)-Menthol	315.7 [9]	12.89 [9]	94.27 [33]	-	-
Benzyl alcohol	257.6 [34]	8.97 [34]	-	-	-
Flavone	369.9 [35]	20.32 [35]	-	-	-
Xylitol	365.7 [36]	37.4 [36]	-	-	-
Meso-erythritol	390.9 [37]	39.4 [37]	-	-	-
Capric acid	304.8 [38]	27.5 [38]	65.74 [39,a]	-	-
Octadecanol	331.34 [40]	65.35 [40]	-	-	-
R-(+)-Camphor	450.4 [14]	5.28	-	III→II: 244 [41] II→I: 369 [41]	III→II: 10 [41] II→I: 0.19 [41]
Lauric acid	317.5 [38]	37.83 [38]	75.33 [39,a]	-	-
4-Nitrophenol	386.34 [42]	11 [42]	-	-	-
Hydroquinone	445.1 [43]	27.23 [43]	-	-	-
Ibuprofen	347.6 [44]	27.94 [44]	50.3 [45]	-	-
Myristic acid	327.03 [38]	41.29 [38]	84.95 [39,a]	-	-
Palmitic acid	336.8 [38]	51.02 [38]	93.99 [39,a]	-	-
Stearic acid	343.7 [38]	61.36 [38]	-	-	-
Octanol	258.34 [46]	25.14 [46]	-	-	-
3-Phenylpropionic acid	321.16 [47]	15.68 [47]	-	-	-
Oleic acid	286.5 [36]	39.6 [36]	-	-	-
Caprylic acid	289.5 [36]	21.38 [36]	-	-	-
Coumarin	342.3 [48]	18.63 [48]	-	-	-
Butylated hydroxytoluene	341.7 [49]	19.87 [49]	-	-	-
Decanol	280 [46]	33.67 [46]	-	-	-
3-Cyclohexylpropionic acid	291.3 [12]	16.96 [12]	-	-	-
Hexadecanol	322.2 [50]	57.74 [50]	-	-	-
Salicylic acid	432.5 [51]	23.05 [51]	-	-	-
Tetradecanol	308.1 [52]	47.29 [52]	-	-	-
Trioctylphosphine oxide	325.9 [7]	58.02 [7]	-	-	-
N,N'-dihexylthiourea	318.7 [16]	20.0 [16]	-	-	-
Phenol	314.15 [53]	11.8635 [53]	64.852 [53]	-	-
Dodecane	263.1 [54]	35.7 [54]	83.38 [55,a]	-	-
Decane	243.1 [36]	28.78 [36]	68.31 [55,a]	-	-
Dodecanol	297.3 [56]	40.307 [56]	-	-	-
2-Phenylethanol	246.2 [22]	9.65 [22]	-	-	-
D-Mannitol	437.3 [57]	54.70 [57]	-	-	-
Sorbitol	366.5 [58]	30.20 [58]	-	-	-
Maltitol	420 [59]	55.10 [59]	-	-	-
Flavanone	348.8 [20]	21.04 [35]	-	-	-
Hesperetin	504.8 [20]	35.9 [60]	-	-	-
Acetylsalicylic acid	407.3 [21]	29.8 [61]	-	-	-
Ketoprofen	367.95 [62]	37.3 [62]	-	-	-
Lidocaine	340.7 [63]	16.4 [63]	-	-	-
Acetaminophen	443.2 [64]	27.6 [64]	-	-	-
(-)-trans-Sobrerol	423.9 [65]	34.81 [65]	-	-	-
(-)-Borneol	481.6 [66]	7.3 [67]	-	II→I: 347.9 [67]	II→I: 3.2 [67]
(±)-Camphene	320.6 [22]	3.12 [22]	-	-	-
1-Methylnaphthalene	242.7 [36]	6.95 [36]	-	-	-
p-Xylene	286.3 [36]	17.11 [36]	-	-	-
Hexadecane	290.7 [54]	53.0 [54]	-	-	-
2,4,6-Trimethylphenol	345.1 [24]	21.41 [24]	-	-	-
2,5-Dimethylphenol	348.1 [68]	13.81 [68]	33.47 [53]	-	-
Dibenzofuran	354.7 [69]	18.6 [69]	-	-	-
Tetracosane	324.1 [36]	54.89 [36]	-	-	-
Naphthalene	353.50 [70]	19.10 [70]	-	-	-
Malonic acid	407.46 [71]	23.1 [71]	-	-	-

Levulinic acid	306.2 [34]	9.22 [34]	-	-	-
Octacosane	334.5 [36]	64.64 [36]	-	-	-
Urea	407.15 [72]	14.60 [72]	7.322 [53]	-	-
Dulcitol	460.3 [36]	46.8 [73]	-	-	-
Myo-Inositol	496.9 [36]	47.9 [36]	-	-	-
Adonitol	374.7 [37]	37.6 [37]	-	-	-
L-Arabitol	374 [74]	43.2 [74]	-	-	-
Fructose (five-membered β-D-Fructose ring enantiomer)	386.8 [75]	33 [76]	120 [77]	-	-
Glucose (six-membered β-Glucose ring enantiomer)	420 [76]	32 [76]	120 [77]	-	-
Sucrose	462.1 [75]	32 [75]	250 [77]	-	-
Octane	216.4 [36]	20.74 [36]	55.28 [55,a]	-	-
2,3-Dimethylphenol	346.0 [34]	21.02 [34]	56.48 [53]	-	-
2,6-Dimethylphenol	318.9 [34]	18.9 [34]	33.47 [53]	-	-
3,4-Dimethylphenol	334.0 [34]	18.13 [34]	35.98 [53]	-	-
3,5-Dimethylphenol	336.8 [34]	18 [34]	33.47 [53]	-	-
Curcumin	446.95 [78]	58.79 [78]	-	-	-
Tyramine	433.6 [79]	28.1 [79]	-	-	-
Water	273.15 [80]	6.01 [80]	-	-	-
Phenylacetic acid	349.2 [45]	15.5 [45]	54.9 [45]	-	-
Benzoic acid	394 [81]	17.3 [81]	-	-	-

[a] Heat capacity differences calculated with experimental data of the solid and liquid phase heat capacities.

Table S.3 – Distribution of the absolute errors of the pure compounds calculated by the GGIC model.

AAD Range (K)	0-5	5-10	10-20
Percentage of compounds	8.1%	5.4%	16.2%
	2,6-Dimethylphenol	1-Methylnaphthalene	2-Phenylethanol
	Acetylsalicylic acid	Benzyl alcohol	Butylated hydroxytoluene
	Camphene	N,N'-dihexylthiourea	Capric acid
	Coumarin	Thymol	Caprylic acid
	Menthol		Flavanone
	Oleic acid		Lauric acid
			Maltitol
			Myristic acid
			Octadecanol
			Palmitic acid
			Stearic acid
			Trioctylphosphine oxide

AAD Range (K)	20-50	50-100	>100
Percentage of compounds	25.7%	27.0%	17.6%
	2,3-Dimethylphenol	2,4,6-Trimethylphenol	4-Nitrophenol
	2,5-Dimethylphenol	3,4-Dimethylphenol	Acetaminophen
	3,5-Dimethylphenol	Adonitol	Borneol
	3-Cyclohexylpropionic acid	Arabitol	Dibenzofuran
	3-Phenylpropionic acid	Flavone	Dulcitol
	Benzoic Acid	Fructose	Glucose
	Curcumin	Hesperetin	Hydroquinone
	Decane	Ibuprofen	Inositol
	Decanol	Ketoprofen	Lidocaine
	Dodecane	Malonic acid	Mannitol
	Dodecanol	Meso-erythritol	Naphthalene
	Hexadecane	Phenol	Sobrerol
	Hexadecanol	Phenylacetic acid	Tyramine
	Levulinic acid	*p*-Xylene	
	Octacosane	R-(+)-Camphor	
	Octane	Sorbitol	
	Octanol	Sucrose	
	Salicylic acid	Tetradecanol	
	Tetracosane	Urea	
		Xylitol	

References

(1) Costa, M. C.; Sardo, M.; Rolemberg, M. P.; Coutinho, J. A. P.; Meirelles, A. J. A.; Ribeiro-Claro, P.; Krähenbühl, M. A. The Solid-Liquid Phase Diagrams of Binary Mixtures of Consecutive, Even Saturated Fatty Acids. *Chem Phys Lipids* **2009**, *160* (2), 85–97. https://doi.org/10.1016/j.chemphyslip.2009.05.004.

(2) Alhadid, A.; Jandl, C.; Mokrushina, L.; Minceva, M. Experimental Investigation and Modeling of Cocrystal Formation in L-Menthol/Thymol Eutectic System. **2021**.

(3) Alhadid, A.; Jandl, C.; Mokrushina, L.; Minceva, M. Nonideality and Cocrystal Formation in L-Menthol/Xylenol Eutectic Systems. *J Mol Liq* **2022**, *367*, 120582. https://doi.org/10.1016/j.molliq.2022.120582.

(4) Abranches, D. O.; Martins, M. A. R.; Silva, L. P.; Schaeffer, N.; Pinho, S. P.; Coutinho, J. A. P. Phenolic Hydrogen Bond Donors in the Formation of Non-Ionic Deep Eutectic Solvents: The Quest for Type v Des. *Chemical Communications* **2019**, *55* (69), 10253–10256.

(5) Florindo, C.; Romero, L.; Rintoul, I.; Branco, L. C.; Marrucho, I. M. From Phase Change Materials to Green Solvents: Hydrophobic Low Viscous Fatty Acid-Based Deep Eutectic Solvents. *ACS Sustain Chem Eng* **2018**, *6* (3), 3888–3895. https://doi.org/10.1021/acssuschemeng.7b04235.

(6) Costa, M. C.; Rolemberg, M. P.; Boros, L. A. D.; Krähenbühl, M. A.; De Oliveira, M. G.; Meirelles, A. J. A. Solid-Liquid Equilibrium of Binary Fatty Acid Mixtures. *J Chem Eng Data* **2007**, *52* (1), 30–36. https://doi.org/10.1021/je060146z.

(7) Schaeffer, N.; Conceição, J. H. F.; Martins, M. A. R.; Neves, M. C.; Pérez-Sánchez, G.; Gomes, J. R. B.; Papaiconomou, N.; Coutinho, J. A. P. Non-Ionic Hydrophobic Eutectics-Versatile Solvents for Tailored Metal Separation and Valorisation. *Green Chemistry* **2020**, *22* (9), 2810–2820.

(8) Haider, M. B.; Jha, D.; Kumar, R.; Marriyappan Sivagnanam, B. Ternary Hydrophobic Deep Eutectic Solvents for Carbon Dioxide Absorption. *International Journal of Greenhouse Gas Control* **2020**, *92* (October 2019), 102839. https://doi.org/10.1016/j.ijggc.2019.102839.

(9) Martins, M. R.; Crespo, E. A.; Pontes, P. V. A.; Silva, L. P.; Bülow, M.; Maximo, G. J.; Batista, E. A. C.; Held, C.; Pinho, S. P.; Coutinho, J. A. P. Tunable Hydrophobic Eutectic Solvents Based on Terpenes and Monocarboxylic Acids. *ACS Sustainable Chemistry & Engineering* **2018**, *6* (7), 8836–8846.

(10) Stott, P. W.; Williams, A. C.; Barry, B. W. Transdermal Delivery from Eutectic Systems: Enhanced Permeation of a Model Drug, Ibuprofen. *Journal of Controlled Release* **1998**, *50* (1–3), 297–308. https://doi.org/10.1016/S0168-3659(97)00153-3.

(11) Okuniewski, M.; Paduszyński, K.; Domańska, U. (Solid + Liquid) Equilibrium Phase Diagrams in Binary Mixtures Containing Terpenes: New Experimental Data and Analysis of Several Modelling Strategies with Modified UNIFAC (Dortmund) and PC-SAFT Equation of State. *Fluid Phase Equilib* **2016**, *422*, 66–77. https://doi.org/10.1016/j.fluid.2015.12.048.

(12) Alhadid, A.; Mokrushina, L.; Minceva, M. Design of Deep Eutectic Systems: A Simple Approach for Preselecting Eutectic Mixture Constituents. *Molecules* **2020**, *25* (5), 1–11. https://doi.org/10.3390/molecules25051077.

(13) Abranches, D. O.; Martins, R. O.; Silva, L. P.; Martins, M. A. R.; Pinho, S. P.; Coutinho, J. A. P. Liquefying Compounds by Forming Deep Eutectic Solvents: A Case Study for Organic Acids and Alcohols. *Journal of Physical Chemistry B* **2020**, *124* (20), 4174–4184.

(14) Martins, M. A. R.; Silva, L. P.; Schaeffer, N.; Abranches, D. O.; Maximo, G. J.; Pinho, S. P.; Coutinho, J. A. P. Greener Terpene-Terpene Eutectic Mixtures as Hydrophobic Solvents. *ACS Sustain Chem Eng* **2019**, *7* (20), 17414–17423. https://doi.org/10.1021/acssuschemeng.9b04614.

(15) Hrynakowski, K.; Szmyt, M. Die Heterogenen Gleichgewichte in Zweistoffsystemen Mit Thymol Als Einer Komponente. *Arch Pharm (Weinheim)* **1935**, *273* (25–28), 418–427. https://doi.org/10.1002/ardp.19352732509.

(16) van den Bruinhorst, A.; Raes, S.; Maesara, S. A.; Kroon, M. C.; Esteves, A. C. C.; Meuldijk, J. Hydrophobic Eutectic Mixtures as Volatile Fatty Acid Extractants. *Sep Purif Technol* **2019**, *216* (September 2018), 147–157. https://doi.org/10.1016/j.seppur.2018.12.087.

(17) Gilmore, M.; McCourt, É. N.; Connolly, F.; Nockemann, P.; Swadźba-Kwaśny, M.; Holbrey, J. D. Hydrophobic Deep Eutectic Solvents Incorporating Trioctylphosphine Oxide: Advanced Liquid Extractants. *ACS Sustain Chem Eng* **2018**, *6* (12), 17323–17332. https://doi.org/10.1021/acssuschemeng.8b04843.

(18) Okuniewski, M.; Paduszyński, K.; Domańska, U. Phase Diagrams in Representative Terpenoid Systems: Measurements and Calculations with Leading Thermodynamic Models. *Ind Eng Chem Res* **2017**, *56* (34), 9753–9761. https://doi.org/10.1021/acs.iecr.7b02207.

(19) Silva, L. P.; Martins, M. A. R.; Abranches, D. O.; Pinho, S. P.; Coutinho, J. A. P. Solid-Liquid Phase Behavior of Eutectic Solvents Containing Sugar Alcohols. *J Mol Liq* **2021**, *337*, 116392. https://doi.org/10.1016/j.molliq.2021.116392.

(20) Teixeira, G.; Abranches, D. O.; Silva, L. P.; Vilas-Boas, S. M.; Pinho, S. P.; Ferreira, A. I. M. C. L.; Santos, L. M. N. B. F.; Ferreira, O.; Coutinho, J. A. P. Liquefying Flavonoids with Terpenoids through Deep Eutectic Solvent Formation. *Molecules* **2022**, *27* (9), 2649. https://doi.org/10.3390/molecules27092649.

(21) Martins, M. A. R.; Silva, L. P.; Jorge, P. S.; Abranches, D. O.; Pinho, S. P.; Coutinho, J. A. P. The Role of Ionic vs. Non-Ionic Excipients in APIs-Based Eutectic Systems. *European Journal of Pharmaceutical Sciences* **2021**, *156* (September 2020), 105583.

(22) Okuniewski, M.; Paduszyński, K.; Domańska, U. Thermodynamic Study of Molecular Interactions in Eutectic Mixtures Containing Camphene. *Journal of Physical Chemistry B* **2016**, *120* (50), 12928–12936. https://doi.org/10.1021/acs.jpcb.6b10034.

(23) De Las Heras, I.; Dufour, J.; Coto, B. A Novel Method to Obtain Solid–Liquid Equilibrium and Eutectic Points for Hydrocarbon Mixtures by Using Differential Scanning Calorimetry and Numerical Integration. *Fuel* **2021**, *297* (October 2020), 120788. https://doi.org/10.1016/j.fuel.2021.120788.

(24) Wang, Y.; Wang, J.; Zhao, X.; Zhu, L.; Yang, L.; Sha, Z. Determination and Thermodynamic Modeling of Solid–Liquid Phase Equilibrium for the 2,4,6-Trimethylphenol and 2,5-Dimethylphenol Binary System. *J Therm Anal Calorim* **2018**, *132* (3), 1923–1931. https://doi.org/10.1007/s10973-018-7117-y.

(25) Hafsaoui, S. L.; Mahmoud, R. Solid-Liquid Equilibria of Binary Systems Containing n-Tetracosane with Naphthalene or Dibenzofuran Prediction with UNIFAC Model. *J Therm Anal Calorim* **2007**, *88* (2), 565–570. https://doi.org/10.1007/s10973-006-8084-2.

(26) Byrne, E. L.; O'Donnell, R.; Gilmore, M.; Artioli, N.; Holbrey, J. D.; Swadźba-Kwaśny, M. Hydrophobic Functional Liquids Based on Trioctylphosphine Oxide (TOPO) and Carboxylic Acids. *Physical Chemistry Chemical Physics* **2020**, *22* (42), 24744–24763. https://doi.org/10.1039/d0cp02605k.

(27) Aşçı, Y. S.; Lalikoglu, M. Development of New Hydrophobic Deep Eutectic Solvents Based on Trioctylphosphine Oxide for Reactive Extraction of Carboxylic Acids. *Ind Eng Chem Res* **2021**, *60* (3), 1356–1365. https://doi.org/10.1021/acs.iecr.0c04551.

(28) Palomo Del Barrio, E.; Cadoret, R.; Daranlot, J.; Achchaq, F. New Sugar Alcohols Mixtures for Long-Term Thermal Energy Storage Applications at Temperatures between 70 °C and 100 °C. *Solar Energy Materials and Solar Cells* **2016**, *155*, 454–468. https://doi.org/10.1016/j.solmat.2016.06.048.

(29) Silva, L.; P.; Fernandez, L.; H. F. Conceição, J.; A.; R. Martins, M.; Sosa, A.; Ortega, J.; P. Pinho, S.; A. P. Coutinho, J. Design and Characterization of Sugar-Based Deep Eutectic Solvents Using Conductor-like Screening Model for Real Solvents. *ACS Sustain Chem Eng* **2018**, *6* (8), 10724–10734.

(30) Gunnam, A.; Nangia, A. K. Solubility Improvement of Curcumin with Amino Acids. *CrystEngComm* **2021**, *23* (18), 3398–3410. https://doi.org/10.1039/d1ce00171j.

(31) Tiecco, M.; Grillo, A.; Mosconi, E.; Kaiser, W.; Del Giacco, T.; Germani, R. Advances in the Development of Novel Green Liquids: Thymol/Water, Thymol/Urea and Thymol/Phenylacetic Acid as Innovative Hydrophobic Natural Deep Eutectic Solvents. *J Mol Liq* **2022**, *364*, 120043. https://doi.org/10.1016/j.molliq.2022.120043.

(32) Zhu, P.; Chen, Y.; Fang, J.; Wang, Z.; Xie, C.; Hou, B.; Chen, W.; Xu, F. Solubility and Solution Thermodynamics of Thymol in Six Pure Organic Solvents. *Journal of Chemical Thermodynamics* **2016**, *92*, 198–206. https://doi.org/10.1016/j.jct.2015.09.010.

(33) Corvis, Y.; Espeau, P. Interpretation of the Global Heat of Melting in Eutectic Binary Systems. *Thermochim Acta* **2018**, *664*, 91–99. https://doi.org/10.1016/j.tca.2018.04.011.

(34) Acree, W. E. Thermodynamic Properties of Organic Compounds: Enthalpy of Fusion and Melting Point Temperature Compilation. *Thermochim Acta* **1991**, *189* (1), 37–56. https://doi.org/10.1016/0040-6031(91)87098-H.

(35) Sousa, C. C. S.; Matos, M. A. R.; Morais, V. M. F. Energetics of Flavone and Flavanone. *Journal of Chemical Thermodynamics* **2009**, *41* (12), 1408–1412. https://doi.org/10.1016/j.jct.2009.06.022.

(36) Domalski, E. S.; Hearing, E. D. Heat Capacities and Entropies of Organic Compounds in the Condensed Phase. Volume III. *J Phys Chem Ref Data* **1996**, *25* (1), 1–525. https://doi.org/10.1063/1.555985.

(37) Barone, G.; Della Gatta, G.; Ferro, D.; Piacente, V. Enthalpies and Entropies of Sublimation, Vaporization and Fusion of Nine Polyhydric Alcohols. *Journal of the Chemical Society, Faraday Transactions* **1990**, *86* (1), 75–79. https://doi.org/10.1039/FT9908600075.

(38) Pontes, P. V. A.; Crespo, E. A.; Martins, A. R.; Silva, L. P.; Pontes, P. V. A.; Crespo, E. A.; Neves, C. M. S. S.; Maximo, G. J.; Dupas, M.; Pinho, P.; Coutinho, A. P.; Sadowski, G.; Batista, E. A. C.; Held, C. Measurement and PC-SAFT Modeling of Solid-Liquid Equilibrium of Deep Eutectic Solvents of Quaternary Ammonium Chlorides and Carboxylic Acids. *Fluid Phase Equilib* **2017**, *448*, 69–80.

(39) Schaake, R. C. F.; van Miltenburg, J. C.; de Kruif, C. G. Thermodynamic Properties of the Normal Alkanoic Acids II. Molar Heat Capacities of Seven Even-Numbered Normal Alkanoic Acids. *J Chem Thermodyn* **1982**, *14* (8), 771–778. https://doi.org/10.1016/0021-9614(82)90173-2.

(40) de Matos, F. C.; da Costa, M. C.; Meirelles, A. J. de A.; Batista, E. A. C. Binary Solid–Liquid Equilibrium Systems Containing Fatty Acids, Fatty Alcohols and Trilaurin by Differential Scanning Calorimetry. *Fluid Phase Equilib* **2016**, *423*, 74–83. https://doi.org/10.1016/j.fluid.2016.04.008.

(41) Rietveld, I. B.; Barrio, M.; Veglio, N.; Espeau, P.; Tamarit, J. L.; Céolin, R. Temperature and Composition-Dependent Properties of the Two-Component System d- and l-Camphor at 'Ordinary' Pressure. *Thermochim Acta* **2010**, *511* (1–2), 43–50. https://doi.org/10.1016/j.tca.2010.07.023.

(42) Musuc, A. M.; Razus, D.; Oancea, D. Investigation of Thermal Stability of Some Nitroaromatic Derivatives by DSC. *Analele Universitatii Bucuresti : Chimie* **2002**, *11* (2), 147–152.

(43) Verevkin, S. P.; Kozlova, S. A. Di-Hydroxybenzenes: Catechol, Resorcinol, and Hydroquinone. *Thermochim Acta* **2008**, *471* (1–2), 33–42. https://doi.org/10.1016/j.tca.2008.02.016.

(44) Hong, J.; Hua, D.; Wang, X.; Wang, H.; Li, J. Solid−Liquid−Gas Equilibrium of the Ternaries Ibuprofen + Myristic Acid + CO 2 and Ibuprofen + Tripalmitin + CO 2. *J Chem Eng Data* **2010**, *55* (1), 297–302. https://doi.org/10.1021/je900342a.

(45) Gracin, S.; Rasmuson, Å. C. Solubility of Phenylacetic Acid, p-Hydroxyphenylacetic Acid, p-Aminophenylacetic Acid, p-Hydroxybenzoic Acid, and Ibuprofen in Pure Solvents. *J Chem Eng Data* **2002**, *47* (6), 1379–1383. https://doi.org/10.1021/je0255170.

(46) van Miltenburg, J. C.; Gabrielová, H.; Růžička, K. Heat Capacities and Derived Thermodynamic Functions of 1-Hexanol, 1-Heptanol, 1-Octanol, and 1-Decanol between 5 K and 390 K. *J Chem Eng Data* **2003**, *48* (5), 1323–1331. https://doi.org/10.1021/je0340856.

(47) Monte, M. J. S.; Hillesheim, D. M. Thermodynamic Study on the Sublimation of 3-Phenylpropionic Acid and of Three Methoxy-Substituted 3-Phenylpropionic Acids. *J Chem Thermodyn* **2001**, *33* (8), 837–847. https://doi.org/10.1006/jcht.2000.0767.

(48) Matos, M. A. R.; Sousa, C. C. S.; Miranda, M. S.; Morais, V. M. F.; Liebman, J. F. Energetics of Coumarin and Chromone. *J Phys Chem B* **2009**, *113* (32), 11216–11221. https://doi.org/10.1021/jp9026942.

(49) Verevkin, S. P. Thermochemistry of Phenols: Buttress Effects in Sterically Hindered Phenols. *J Chem Thermodyn* **1999**, *31* (11), 1397–1416. https://doi.org/10.1006/jcht.1999.0466.

(50) Xing, J.; Tan, Z.-C.; Shi, Q.; Tong, B.; Wang, S.-X.; Li, Y.-S. Heat Capacity and Thermodynamic Properties of 1-Hexadecanol. *J Therm Anal Calorim* **2008**, *92* (2), 375–380. https://doi.org/10.1007/s10973-007-8955-1.

(51) Peña, M. A.; Escalera, B.; Reíllo, A.; Sánchez, A. B.; Bustamante, P. Thermodynamics of Cosolvent Action: Phenacetin, Salicylic Acid and Probenecid. *J Pharm Sci* **2009**, *98* (3), 1129–1135. https://doi.org/10.1002/jps.21497.

(52) Zeng, J. L.; Cao, Z.; Yang, D. W.; Xu, F.; Sun, L. X.; Zhang, L.; Zhang, X. F. Phase Diagram of Palmitic Acid-Tetradecanol Mixtures Obtained by DSC Experiments. *J Therm Anal Calorim* **2009**, *95* (2), 501–505. https://doi.org/10.1007/s10973-008-9274-x.

(53) Jamroz, M. E.; Palczewska-Tulinska, M.; Wyrzykowska-Stankiewicz, D.; Szafranski, A. M.; Polaczek, J.; Cz Dobrowolski, J.; Jamroz, M. H.; Mazurek, A. P. *The Urea-Phenol s Systems*; 1998; Vol. 152.

(54) Mondieig, D.; Rajabalee, F.; Metivaud, V.; Oonk, H. A. J.; Cuevas-Diarte, M. A. N -Alkane Binary Molecular Alloys. *Chemistry of Materials* **2004**, *16* (5), 786–798. https://doi.org/10.1021/cm031169p.

(55) Finke, H. L.; Gross, M. E.; Waddington, G.; Huffman, H. M. Low-Temperature Thermal Data for the Nine Normal Paraffin Hydrocarbons from Octane to Hexadecane. *J Am Chem Soc* **1954**, *76* (2), 333–341. https://doi.org/10.1021/ja01631a005.

(56) van Miltenburg, J. C.; van den Berg, Gerrit. J. K.; Ramirez, M. Heat Capacities and Derived Thermodynamic Functions of 1-Dodecanol and 1-Tridecanol between 10 K and 370 K and Heat Capacities of 1-Pentadecanol and 1-Heptadecanol between 300 K and 380 K and Correlations for the Heat Capacity and the Entropy of Liquid n. *J Chem Eng Data* **2003**, *48* (1), 36–43. https://doi.org/10.1021/je025524o.

(57) Tong, B.; Liu, R.-B.; Meng, C.-G.; Yu, F.-Y.; Ji, S.-H.; Tan, Z.-C. Heat Capacities and Nonisothermal Thermal Decomposition Reaction Kinetics of D-Mannitol. *J Chem Eng Data* **2010**, *55* (1), 119–124. https://doi.org/10.1021/je900285w.

(58) Barone, G.; Gatta, G. Della; Ferro, D.; Piacente, V. Enthalpies and Entropies of Sublimation, Vaporization and Fusion of Nine Polyhydric Alcohols. *Journal of the Chemical Society, Faraday Transactions* **1990**, *86* (1), 75. https://doi.org/10.1039/ft9908600075.

(59) Lebrun, N.; Van Miltenburg, J. C.; Bustin, O.; Descamps, M. Calorimetric Fragility of Maltitol. *Phase Transitions* **2003**, *76* (9–10), 841–846. https://doi.org/10.1080/0141159031000085723.

(60) Chebil, L.; Humeau, C.; Anthoni, J.; Dehez, F.; Engasser, J.-M.; Ghoul, M. Solubility of Flavonoids in Pure Solvents. *J Chem Eng Data* **2007**, *52*, 1552–1556.

(61) Kirklin, D. R. Enthalpy of Combustion of Acetylsalicylic Acid. *J Chem Thermodyn* **2000**, *32* (6), 701–709. https://doi.org/10.1006/jcht.1999.0650.

(62) Wassvik, C. M.; Holmén, A. G.; Bergström, C. A. S.; Zamora, I.; Artursson, P. Contribution of Solid-State Properties to the Aqueous Solubility of Drugs. *European Journal of Pharmaceutical Sciences* **2006**, *29* (3–4), 294–305. https://doi.org/10.1016/j.ejps.2006.05.013.

(63) Lazerges, M.; Rietveld, I. B.; Corvis, Y.; Céolin, R.; Espeau, P. Thermodynamic Studies of Mixtures for Topical Anesthesia: Lidocaine-Salol Binary Phase Diagram. *Thermochim Acta* **2010**, *497* (1–2), 124–128. https://doi.org/10.1016/j.tca.2009.08.016.

(64) Mota, F. L.; Carneiro, A. P.; Queimada, A. J.; Pinho, S. P.; Macedo, E. A. Temperature and Solvent Effects in the Solubility of Some Pharmaceutical Compounds: Measurements and Modeling. *European Journal of Pharmaceutical Sciences* **2009**, *37* (3–4), 499–507. https://doi.org/10.1016/j.ejps.2009.04.009.

(65) Bettinetti, G.; Giordano, F.; Fronza, G.; Italia, A.; Pellegata, R.; Villa, M.; Ventura, P. Sobrerol Enantiomers and Racemates: Solid-State Spectroscopy, Thermal Behavior, and Phase Diagrams. *J Pharm Sci* **1990**, *79* (6), 470–475. https://doi.org/10.1002/jps.2600790603.

(66) Chandra, G.; Murthy, S. S. N. Dielectric and Thermodynamic Study of Camphor and Borneol Enantiomers and Their Binary Systems. *Thermochim Acta* **2018**, *666*, 241–252. https://doi.org/10.1016/j.tca.2018.04.014.

(67) Štejfa, V.; Fulem, M.; Růžička, K.; Červinka, C. Thermodynamic Study of Selected Monoterpenes II. *J Chem Thermodyn* **2014**, *79*, 272–279. https://doi.org/10.1016/j.jct.2013.12.012.

(68) Jamróz, M. E.; Palczewska-Tulińska, M.; Wyrzykowska-Stankiewicz, D.; Szafrański, A. M.; Polaczek, J.; Dobrowolski, J. Cz.; Jamróz, M. H.; Mazurek, A. P. The Urea–Phenol(s) Systems. *Fluid Phase Equilib* **1998**, *152* (2), 307–326. https://doi.org/10.1016/S0378-3812(98)90206-0.

(69) Kestens, V.; Auclair, G.; Drozdzewska, K.; Held, A.; Roebben, G.; Linsinger, T. Thermodynamic Property Values of Selected Polycyclic Aromatic Hydrocarbons Measured by Differential Scanning Calorimetry. *J Therm Anal Calorim* **2010**, *99* (1), 245–261. https://doi.org/10.1007/s10973-009-0440-6.

(70) Sharma, B. L.; Gupta, S.; Tandon, S.; Kant, R. Physico-Mechanical Properties of Naphthalene–Acenaphthene Eutectic System by Different Modes of Solidification. *Mater Chem Phys* **2008**, *111* (2–3), 423–430. https://doi.org/10.1016/j.matchemphys.2008.04.049.

(71) Hansen, A. R.; Beyer, K. D. Experimentally Determined Thermochemical Properties of the Malonic Acid/Water System: Implications for Atmospheric Aerosols. *J Phys Chem A* **2004**, *108* (16), 3457–3466. https://doi.org/10.1021/jp0376166.

(72) Rai, U. S.; Rai, R. N. *Some Physicochemical Studies on Organic Eutectics and Molecular Complex: Urea-p-Nitrophenol System*; 1999.

(73) Solé, A.; Neumann, H.; Niedermaier, S.; Cabeza, L. F.; Palomo, E. Thermal Stability Test of Sugar Alcohols as Phase Change Materials for Medium Temperature Energy Storage Application. In *Energy Procedia*; Elsevier Ltd, 2014; Vol. 48, pp 436–439. https://doi.org/10.1016/j.egypro.2014.02.051.

(74) Carpentier, L.; Desprez, S.; Descamps, M. Crystallization and Glass Properties of Pentitols: Xylitol, Adonitol, Arabitols. *J Therm Anal Calorim* **2003**, *73* (2), 577–586. https://doi.org/10.1023/A:1025482230325.

(75) Hurtta, M.; Pitkänen, I.; Knuutinen, J. Melting Behaviour of D-Sucrose, d-Glucose and d-Fructose. *Carbohydr Res* **2004**, *339* (13), 2267–2273. https://doi.org/10.1016/j.carres.2004.06.022.

(76) van Putten, R.-J.; Winkelman, J. G. M.; Keihan, F.; van der Waal, J. C.; de Jong, E.; Heeres, H. J. Experimental and Modeling Studies on the Solubility of d -Arabinose, d -Fructose, d -Glucose, d -Mannose, Sucrose and d -Xylose in Methanol and Methanol–Water Mixtures. *Ind Eng Chem Res* **2014**, *53* (19), 8285–8290. https://doi.org/10.1021/ie500576q.

(77) Ferreira, O.; Brignole, E. A.; Macedo, E. A. Phase Equilibria in Sugar Solutions Using the A-UNIFAC Model. In *Industrial and Engineering Chemistry Research*; American Chemical Society, 2003; Vol. 42, pp 6212–6222. https://doi.org/10.1021/ie030246n.

(78) Kakran, M.; Sahoo, N. G.; Tan, I. L.; Li, L. Preparation of Nanoparticles of Poorly Water-Soluble Antioxidant Curcumin by Antisolvent Precipitation Methods. *Journal of Nanoparticle Research* **2012**, *14* (3). https://doi.org/10.1007/s11051-012-0757-0.

(79) Huxoll, F.; Heyng, M.; Andreeva, I. V.; Verevkin, S. P.; Sadowski, G. Thermodynamic Properties of Biogenic Amines and Their Solutions. *J Chem Eng Data* **2021**, *66* (7), 2822–2831. https://doi.org/10.1021/acs.jced.1c00202.

(80) Eisenberg, D.; Kauzmann, W. *The Structure and Properties of Water*; Clarendon Press: Oxford, 1969.

(81) Sharma, B. L.; Kant, R.; Sharma, R.; Tandon, S. Deviations of Binary Organic Eutectic Melt Systems. *Mater Chem Phys* **2003**, *82* (1), 216–224. https://doi.org/10.1016/S0254-0584(03)00199-8.